Loss of Roquin induces early death and immune deregulation but not autoimmunity

Arianna Bertossi,[1] Martin Aichinger,[2] Paola Sansonetti,[1] Maciej Lech,[3] Frauke Neff,[4] Martin Pal,[5,6] F. Thomas Wunderlich,[5,6] Hans-Joachim Anders,[3] Ludger Klein,[2] and Marc Schmidt-Supprian[1]

[1]Max Planck Institute of Biochemistry, 82152 Martinsried, Germany
[2]Institute for Immunology, Ludwig-Maximilians University, 80336 Munich, Germany
[3]Nephrological Center, Medical Policlinic, University of Munich, 80336 Munich, Germany
[4]Helmholtz Center Munich, 85764 Neuherberg, Germany
[5]Institute for Genetics, University of Cologne, 50674 Cologne, Germany
[6]Max Planck Institute for Neurological Research, 50931 Cologne, Germany

The substitution of one amino acid in the Roquin protein by the sanroque mutation induces a dramatic autoimmune syndrome in mice. This is believed to occur through ectopic expression of inducible T cell co-stimulator (ICOS) and unrestrained differentiation of follicular T helper cells, which induce spontaneous germinal center reactions to self-antigens. In this study, we demonstrate that tissue-specific ablation of Roquin in T or B cells, in the entire hematopoietic system, or in epithelial cells of transplanted thymi did not cause autoimmunity. Loss of Roquin induced elevated expression of ICOS through T cell–intrinsic and –extrinsic mechanisms, which itself was not sufficient to break self-tolerance. Instead, ablation of Roquin in the hematopoietic system caused defined changes in immune homeostasis, including the expansion of macrophages, eosinophils, and T cell subsets, most dramatically CD8 effector–like T cells, through cell-autonomous and nonautonomous mechanisms. Germline Roquin deficiency led to perinatal lethality, which was partially rescued on the genetic background of an outbred strain. However, not even complete absence of Roquin resulted in overt self-reactivity, suggesting that the sanroque mutation induces autoimmunity through an as yet unknown mechanism.

CORRESPONDENCE
Marc Schmidt-Supprian:
supprian@biochem.mpg.de

Abbreviations used: ANOVA, analysis of variance; ES, embryonic stem; ICOS, inducible T cell co-stimulator; MFI, mean fluorescence intensity; mRNA, messenger RNA; PAS, periodic acid Schiff.

Autoimmunity occurs when immune effector mechanisms, normally used to protect organisms against invading pathogens, are unleashed onto self-constituents. Most autoimmune diseases are complex, multifactorial processes, reflecting the number and the nature of checkpoints that have to be overcome (Goodnow, 2007).

Only a small number of critical proteins appear to play such central roles in the maintenance of immunological self-tolerance that alterations in their function strongly predispose to a rapid development of autoimmune syndromes. Vinuesa et al. (2005) identified the M199R amino acid substitution in the putative E3 ubiquitin ligase Roquin/Rc3h1 as the cause of the spontaneous lupus-like autoimmune disease characterizing the *sanroque* mouse strain. *san/san* mice display splenomegaly, lymphadenopathy, plasmacytosis, spontaneous germinal center formation, and glomerulonephritis with immune complex deposition. High affinity anti-DNA autoantibodies can be detected as early as 6 wk after birth (Vinuesa et al., 2005). The dominant disease-preventing mechanism of Roquin is thought to be the inhibition of inappropriate inducible T cell co-stimulator (ICOS) expression on T cells (Linterman et al., 2009a; Yu and Vinuesa, 2010) through direct ICOS messenger RNA (mRNA) binding and targeting to P-bodies and components of the decapping machinery (Athanasopoulos et al., 2010; Glasmacher et al., 2010). The M199R *sanroque* mutation is located in a novel protein domain termed ROQ, which so far has been identified only in Roquin and its paralogue Mnab. The ROQ domain is critical for ICOS mRNA binding and repression. Because the M199R mutation does not affect binding to ICOS mRNA, it has been postulated that it interferes with Roquin's

The Rockefeller University Press $30.00
J. Exp. Med. Vol. 208 No. 9 1749-1756
www.jem.org/cgi/doi/10.1084/jem.20110578

The Journal of Experimental Medicine

ability to interact with as yet unknown critical effector proteins (Athanasopoulos et al., 2010).

ICOS is an essential co-stimulatory receptor for follicular T helper cell differentiation (King et al., 2008), and heterozygous ablation of ICOS (Yu et al., 2007) or depletion of follicular T helper cells each significantly reduces the autoimmune manifestations in *san/san* mice. Adoptive transfer of *san/san* follicular T helper cells induces spontaneous germinal center formation in recipient mice (Linterman et al., 2009b). Collectively, these data led to the current concept that the *sanroque* mutation induces accumulation and dysregulation of follicular helper T cells through T cell–intrinsic mechanisms, which in turn drive aberrant positive selection of autoreactive B cells in the germinal center with ensuing autoimmunity (Yu and Vinuesa, 2010). To study the tissue-specific function of Roquin in mouse physiology and autoimmune reactions, we generated a conditional Roquin knockout (*rc3h1*^{F}) allele.

RESULTS AND DISCUSSION

Complete Roquin knockout causes perinatal lethality

To allow tissue-specific ablation of Roquin, we flanked exons 4–6 of the *Rc3h1* gene with loxP sites (Fig. S1 A). The genetic background of the gene-targeted embryonic stem (ES) cells and all Cre transgenic mice used for tissue-specific gene ablation of Roquin was C57BL/6. Western blotting using *Rc3h1*$^{F/F}$ embryonic fibroblasts, in which exons 4–6 had been excised by cre protein transduction, demonstrated the generation of a true Roquin-null mutation (Fig. 1 A). A conventional Roquin knockout strain was produced through crosses with a germline cre-deleter strain. Roquin$^{-/-}$ pups were born at Mendelian ratios (Fig. 1 B) but died within 6 h after birth. Roquin$^{-/-}$ mice displayed a curly tail (Fig. 1 C) and malformations of the caudal spinal column (Fig. 1 D), which is often seen in mutant mice with delayed or abnormal neural tube closure (Harris and Juriloff, 2007). The death of the animals might be related to impaired lung function because the alveoli were not properly expanded in the lungs of Roquin-deficient pups (Fig. 1 E). Besides this, we could not detect obvious structural problems or indications of an acute respiratory distress syndrome in the lungs of Roquin$^{-/-}$ mice.

Ablation of Roquin in the T lineage leads to elevated ICOS levels and expansion of effector CD8 T cells but not autoimmunity

The lupus-like symptoms in *san/san* mice have been ascribed to a T cell–intrinsic function of Roquin (Linterman et al., 2009a,b). To address whether ablation of Roquin specifically in T cells would recapitulate the effects of the *sanroque* mutation, we generated *CD4cre/Rc3h1*^{FlF} (T$^{\Delta Rc3h1}$) mice. As expected, Roquin deficiency led to a robust up-regulation of ICOS on all T cell subsets in thymus and secondary lymphoid organs (Fig. 2 A and Fig. S1 B). Loss of Roquin (Fig. S1 C) did not affect T cell development or subset composition in the thymus (Fig. S1 D). In peripheral lymphoid organs, there was a significant increase in CD8 but not CD4 T cells that displayed an effector-like phenotype (CD44^{hi}CD62L^{lo}; Fig. 2, B and D; and Fig. S2 A). Further analysis of the CD44^{hi}CD62L^{lo} CD8 T cells revealed that most of them were CD127^{int}CD122^{hi}KLRG1^{hi}Tbet^{hi} (Fig. 2 C and Fig. S2 C) and therefore resembled short-lived effector cells. T$^{\Delta Rc3h1}$ mice had normal-sized spleens with regular follicular organization (Fig. S2, B and D), although the numbers of eosinophils and monocytic/macrophage populations were doubled compared with control mice (Fig. 2 D). Most importantly, unlike what is seen in *san/san* mice (Vinuesa et al., 2005), we neither detected increased follicular T helper cell differentiation (Fig. S2 E) nor spontaneous germinal center formation (Fig. 2 E and Fig. S2 E). T$^{\Delta Rc3h1}$ mice did not display any obvious autoimmune manifestations, including the production of autoantibodies (Fig. S2 F). We therefore conclude that the absence of Roquin specifically in T cells leads to the up-regulation of ICOS expression and expansion of CD8 effector phenotype T cells but not to aberrant follicular T helper cell differentiation or break of tolerance to self.

Roquin deficiency in hematopoietic cells causes immune deregulation

Because T cell–specific ablation of Roquin was not sufficient to recapitulate the dramatic breakdown of self-tolerance seen

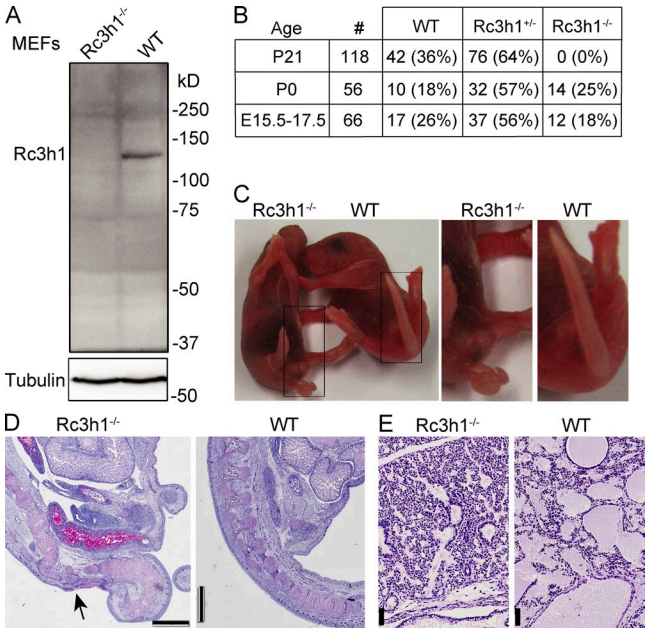

Figure 1. Loss of Roquin causes perinatal lethality. (A) Western blot of Roquin protein expression in wild-type and *Rc3h1*$^{-/-}$ immortalized murine embryonic fibroblasts. (B) Genotype frequency of offspring from intercrosses of *Rc3h1*$^{+/-}$ mice. (C) Newborn (P0) *Rc3h1*$^{-/-}$ pups show a curly tail. (D) PAS stainings of sagittal sections of the sacral spinal column of *Rc3h1*$^{-/-}$ and control newborn mice; the arrow indicates the skin, soft tissue, and bone defect. (E) PAS stainings of sagittal sections of lungs of *Rc3h1*$^{-/-}$ and control newborn mice. Bars: (D) 1 mm; (E) 50 µm.

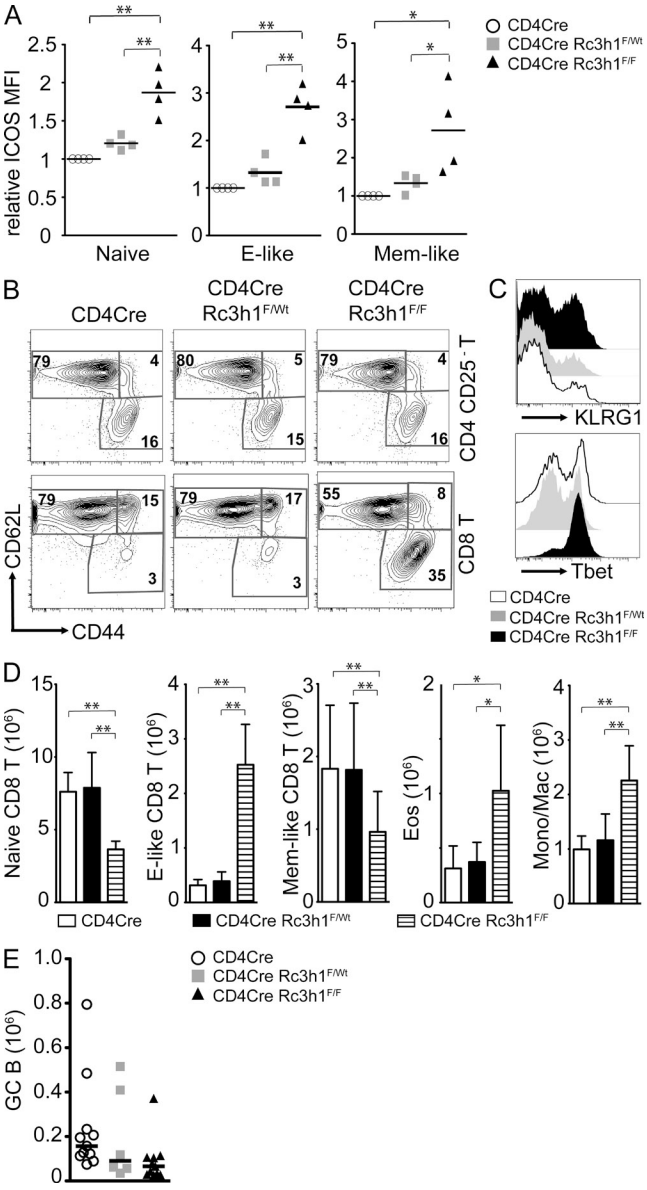

Figure 2. Roquin deficiency in T lymphocytes leads to CD8 effector–like T cell expansion. (A) Relative MFI of ICOS expression on CD4 T cell subsets in the spleens of mice of the indicated genotypes. Naive, $CD25^{-}CD44^{lo}CD62L^{hi}$; effector (E)-like, $CD25^{-}CD44^{hi}CD62L^{lo}$; memory (Mem)-like, $CD25^{-}CD44^{hi}CD62L^{hi}$. Bars indicate medians of four mice per group, and ICOS levels on CD4cre control T cell subsets are set to 1. (B) Representative contour plots of T cell (TCR-β^{+}) subsets gated as indicated on the right. Numbers represent percentages of the gated populations of the indicated T cell subtype. (C) Histogram of KLRG1 and Tbet expression on $CD44^{hi}CD62L^{lo}$-gated effector-like CD8 T cells, representative of five experiments. (D) Bar charts of absolute numbers of indicated T cell (TCR-β^{+}; subsets as in A) and myeloid cell subsets: Eos, eosinophils ($Gr1^{int}SiglecF^{+}$); Mono/Mac, monocytes/macrophages ($SiglecF^{-}Gr1^{int}Mac1^{+}$). Columns and error bars indicate means ± SD calculated from six to nine mice per genotype. (E) Absolute numbers of splenic germinal center (GC; $B220^{+}PNA^{hi}Fas^{hi}CD38^{lo}$) B cells of 11–6 mice per genotype. Bars indicate the median. *, $P < 0.05$; **, $P < 0.001$; one-way ANOVA.

in *san/san* mice, we hypothesized that loss of Roquin in other hematopoietic cells might synergize with its absence in T cells to induce autoimmunity. We therefore generated *VavCre/Roquin*$^{F/F}$ ($Hem^{\Delta Rc3h1}$) mice to test the consequences of Roquin deficiency in the entire hematopoietic system (Fig. 3 A). $Hem^{\Delta Rc3h1}$ mice displayed normal T cell development in the thymus (Fig. S3 A), whereas BM B cell development was affected through a reduction in immature and recirculating B cells (Fig. S3 B). Spleen size and cellular content were increased ∼1.5-fold as the result of expansion of effector-like T cells, $Foxp3^{+}$ regulatory T cells (T_{reg} cells), eosinophils, and monocytic/macrophage populations (Fig. 3, B–D; and Fig. S3, C and D). However, the increased splenic cellularity in $Hem^{\Delta Rc3h1}$ mice did not reach the extent of splenomegaly observed in *san/san* mice, which occurs independently of the autoimmune syndrome (Linterman et al., 2009b). Analysis of splenic immune compartmentalization by immunofluorescence revealed both intact and somewhat disrupted (Fig. 3 E) follicles in $Hem^{\Delta Rc3h1}$ mice. Moreover, we detected an increase in spontaneous germinal center formation in the spleens of $Hem^{\Delta Rc3h1}$ mice (Fig. 3 G). Analysis of Ig serum levels by ELISA revealed a reduction in IgG1, IgG3, and IgA and an increase in IgG2b levels (Fig. S4 A). However, we did not detect elevated levels of autoantibodies in the serum of $Hem^{\Delta Rc3h1}$ mice by ELISA for typical autoantigens (Fig. 3 H and Fig. S4 B) or by staining of kidney, harderian gland, and stomach sections of $Rag2^{-/-}$ mice (not depicted). Importantly, there was no autoimmune tissue damage in kidney, liver, and lung of $Hem^{\Delta Rc3h1}$ mice (not depicted).

Of note, the extent of ICOS up-regulation on CD4 and, to a lesser extent, CD8 T cells in $Hem^{\Delta Rc3h1}$ mice exceeded the increase of ICOS levels in $T^{\Delta Rc3h1}$ mice (compare Fig. 3 F and Fig. S4 C with Fig. 2 A and Fig. S1 B). This suggests that the loss of Roquin in immune cells other than T cells contributes to the elevated ICOS expression in $Hem^{\Delta Rc3h1}$ mice. Along the same lines, no corresponding increase of regulatory or effector-like CD4 T cells had been observed upon T cell–specific ablation of Roquin, indicating that these alterations reflect a requirement for Roquin outside the T lineage.

Roquin-deficient B cells contribute to the general deregulation of immune homeostasis

To elucidate to which extent loss of Roquin function specifically in B cells contributes to the immune activation observed in $Hem^{\Delta Rc3h1}$ mice, we generated *CD19cre/Rc3h1*$^{F/F}$ ($B^{\Delta Rc3h1}$) mice. Ablation of Roquin specifically in B lymphocytes (Fig. S4 D) was sufficient to cause enlarged spleens (Fig. S4 E) resulting from the expansion of B cells, T_{reg} cells, CD4 and CD8 effector–like T cells, and eosinophils (Fig. 4 A and Fig. S4, F–I). There was a trend toward elevated spontaneous germinal center formation in the spleens of $B^{\Delta Rc3h1}$ mice, but the observed differences were not statistically significant (Fig. 4 B). Therefore, our findings show that lack of Roquin in B cells contributed significantly to the disturbance of immune homeostasis in $Hem^{\Delta Rc3h1}$ mice.

Roquin deficiency in thymic epithelial cells causes thymic atrophy but does not affect T cell selection

Loss of Roquin in hematopoietic cells does not cause a dramatic *sanroque*-like autoimmune syndrome. We therefore hypothesized that Roquin-deficient nonhematopoietic cells might be crucial for the induction of autoimmunity. The thymic epithelium plays a critical role for immune tolerance, and perturbations of its development and/or function can lead to spontaneous autoimmunity (Kyewski and Klein, 2006). To assess the function of Roquin specifically in thymic epithelial cells during thymocyte development and selection, we transplanted immune cell–depleted Roquin-deficient and control embryonic thymi under the kidney capsule of athymic C57BL/6 nude mice. As a consequence, these chimeras contained a Roquin-sufficient hematopoietic system, and T cells were selected on either Roquin-deficient ($Rc3h1^{-/-}$ → nude) or -sufficient ($Rc3h1^{+/+}$ → nude) thymic epithelium. Recipients of Roquin-deficient thymic epithelium gained weight normally after transplantation (Fig. 5 A) and did not show signs of disease by histological criteria (not depicted). Embryonic day (E) 16.5 $Rc3h1^{-/-}$ thymic lobes at the time of grafting appeared somewhat smaller than $Rc3h1^{+/+}$ controls, and the cellularity of $Rc3h1^{-/-}$ thymi 10 wk after transplantation was significantly reduced compared with controls (Fig. 5 B). Despite this thymic atrophy, which points to a thymic epithelium–intrinsic function of Roquin in epithelial homeostasis, thymocyte development was not affected (Fig. 5 C). T cell selection was also unaffected, as judged from the normal numbers of

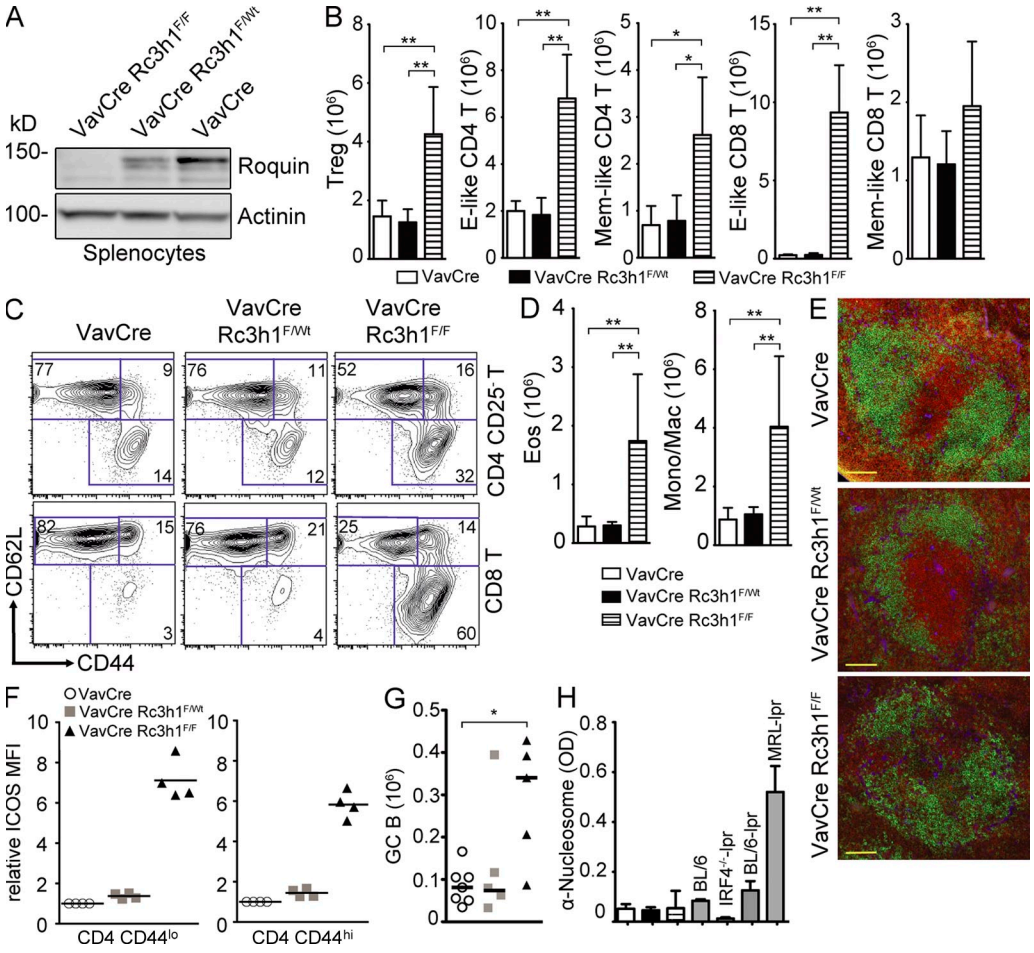

Figure 3. Deregulation of immune homeostasis in the absence of Roquin in the hematopoietic system. (A) Western blot analysis to evaluate Roquin protein expression in splenocytes. (B and C) Absolute cell numbers (B) and representative contour plots (C) of splenic T cell (TCR-β^+) subsets: effector (E)-like, $CD44^{hi}CD62L^{lo}$; and memory (Mem)-like, $CD44^{hi}CD62L^{hi}$ (n = 7–9); T_{reg} cells, $CD4^+FoxP3^+$ (n = 3–5). Columns and error bars represent means ± SD calculated from the number of mice indicated. (D) Columns and error bars represent means ± SD of absolute cell numbers of eosinophils (Eos; $Gr1^{int}SiglecF^+$) and monocytic/macrophages (Mono/Mac; $SiglecF^-Gr1^{int}Mac1^+$) calculated from four to six mice per group. (E) Immunofluorescence of spleen sections: green, α-B220; red, α-CD3; blue, α-laminin. Bars, 100 µm. (F) Relative ICOS MFI of naive ($CD44^{lo}$) and memory/effector-like ($CD44^{hi}$) splenic CD4 T cells. Bars indicate medians. (G) Absolute cell numbers of germinal center (GC; $B220^+PNA^{hi}Fas^{hi}CD38^{lo}$) B cells. Bars represent medians calculated from five to seven mice per genotype. (H) Titers of serum autoantibodies against nucleosomes measured by ELISA (2–7 mo old) from 8–10 mice of the indicated genotypes. Sera from BL/6, $IRF4^{-/-}$-lpr, BL/6-lpr, and MRL-lpr mice were used as positive or negative controls. Columns and error bars represent means ± SD. *, $P < 0.05$; **, $P < 0.001$; one-way ANOVA.

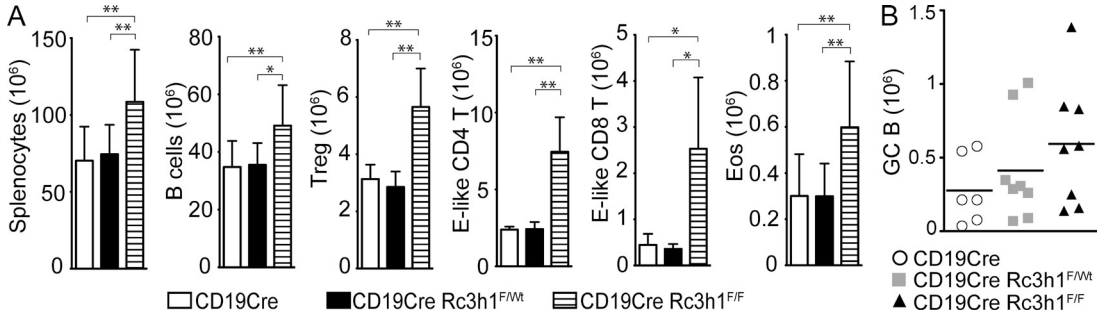

Figure 4. Roquin-deficient B cells cause effector-like T cell expansion. (A) Column and error bars represent means ± SD of absolute cell numbers of splenocytes ($n = 8$), B cells ($B220^+$; $n = 8$), T_{reg} cells ($CD4^+FoxP3^+$; $n = 4$), CD4 effector (E)–like T cells ($CD25^-CD44^{hi}CD62L^{lo}$; $n = 4$), CD8 effector–like T cells ($CD44^{hi}CD62L^{lo}$; $n = 4$), and eosinophils (Eos; $Gr1^{int}SiglecF^+$; $n = 8$). (B) Absolute cell numbers of germinal center (GC; $B220^+Fas^{hi}PNA^{hi}CD38^{lo}$) B cells. Bars indicate medians calculated from six to eight mice per group. *, $P < 0.05$; **, $P < 0.001$; one-way ANOVA.

peripheral T cell subsets (Fig. S5 A) and normal proportions of TCRs bearing certain α and β chains (Fig. 5 D and Fig. S5 B). These data show that although absence of Roquin in the thymic epithelium reduced thymus size under these experimental conditions, it did not affect T cell selection or allow the escape of self-reactive T cells.

CD1 outbred Roquin$^{-/-}$ mice survive at sub-Mendelian ratios and display growth retardation and relatively mild immune defects

To overcome the perinatal lethality that prevents the analysis of adult C57BL/6 Roquin-deficient mice, we crossed C57BL/6 Roquin$^{+/-}$ mice onto a CD1 outbred background. 4% of CD1 Roquin$^{-/-}$ mice survived to adulthood (Fig. 6 A) in heterozygous crosses, displaying growth retardation (Fig. 6 B) and the typical curly tail at birth, which was sometimes corrected later on (Fig. S6 A). In general, the immune phenotypes were somewhat milder in CD1 Roquin$^{-/-}$ than in C57BL/6 Hem$^{\Delta Rc3h1}$ mice, most likely because of the CD1 outbred background. CD1 Roquin$^{-/-}$ mice displayed enlarged spleens (Fig. S6 B) with a trend toward increased numbers of eosinophils and monocytic/macrophage populations (Fig. 6 C and Fig. S6 C). However, the most prominent effect was a dramatic and selective expansion of Roquin-deficient CD8 effector–like T cells (Fig. 6 C), showing that suppressing the generation of these cells is a dominant function of Roquin in naive mice. Splenic follicular organization was normal (Fig. 6 D), and the numbers of CD4 T cell subtypes and B cells (Fig. S6 D) were not significantly altered in CD1 Roquin$^{-/-}$ mice. In addition, we did not detect spontaneous germinal center formation (Fig. 6 E), autoantibody production (Fig. 6 F and Fig. S6 E), or autoimmune tissue damage in CD1 Roquin$^{-/-}$ mice (not depicted).

We show in this study that, unlike the *sanroque* mutation, systemic ablation of Roquin causes perinatal lethality, revealing a hitherto unappreciated critical role of Rc3h1 outside the immune system. In immune cells, loss of Roquin induces several defined perturbations. Deficiency in B cells leads to elevated numbers of B, regulatory and effector-like T cells, and eosinophils. Roquin deletion in T cells induces the expansion of eosinophils and macrophages and the dramatic spontaneous differentiation of effector-like CD8 T cells. Our findings

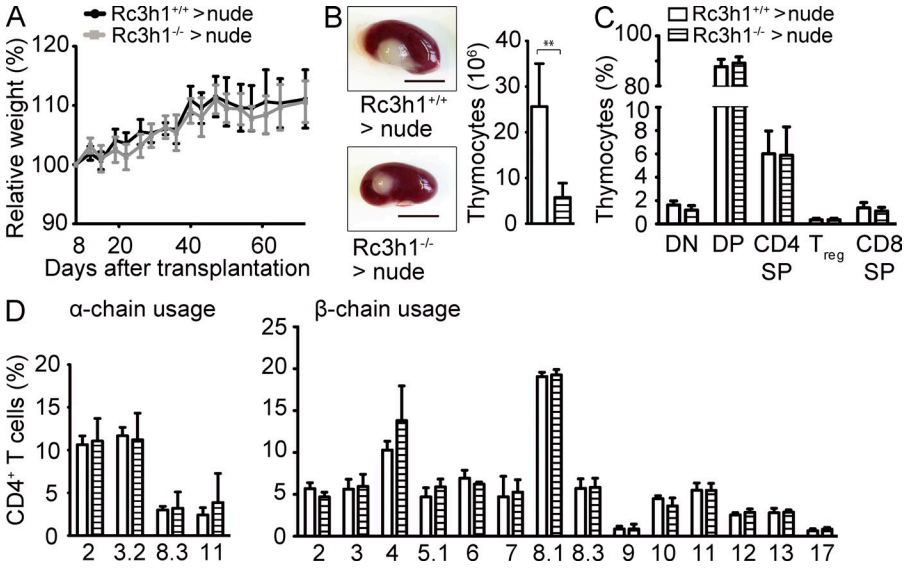

Figure 5. Effect of Roquin loss in thymic epithelial cells. (A) Growth curve of nude mice transplanted with fetal thymic epithelium as indicated. Means ± SD for recipients of six wild-type and six *Rc3h1*$^{-/-}$ thymi are shown. (B) *Rc3h1*$^{+/+}$ and *Rc3h1*$^{-/-}$ thymic epithelium–derived thymus lobes on kidneys of C57BL/6 nude mice 10 wk after transplantation. Bar chart shows absolute numbers of thymocytes. Bars, 500 µm. (C) Proportions of thymocyte subsets. DN, (CD4/CD8) double negative; DP, double positive; SP, single positive; T_{reg} cells, $CD4^+FoxP3^+$. (D) Usage of individual Vα (left) and Vβ (right) chains in the TCR on CD4 T cells in mice of the indicated genotypes. (B–D) Columns and error bars represent means ± SD of five to six mice per group. **, $P < 0.001$; Student's *t* test.

clearly demonstrate that ablation of Roquin, although it augments ICOS expression levels through T cell–autonomous and nonautonomous mechanisms, is not sufficient to cause autoimmunity. It remains possible that C57BL/6 complete Roquin knockout mice would develop a *sanroque*-like autoimmune syndrome if the perinatal lethality could be overcome by some means. However, it seems more likely that the *sanroque* mutation causes to date unidentified perturbations, which are not recapitulated by the absence of Roquin. In this scenario, another protein such as the Roquin paralogue Mnab might compensate for the absence of Roquin, which it cannot do in the presence of $Roquin_{M199R}$. Therefore, the presence of $Roquin_{M199R}$ in protein complexes might be more disruptive than the absence of the protein. This hypothesis is supported by the fact that heterozygous C57BL/6 san/WT (Vinuesa et al., 2005), but not C57BL/6 $Roquin^{+/-}$ (Fig. S6 F) animals develop antinuclear autoantibodies. Be this as it may, our findings show that to bring about a spontaneous failure of immune tolerance, a complex and as yet ill-defined interplay of Roquin absence or malfunction in various cell types may be required.

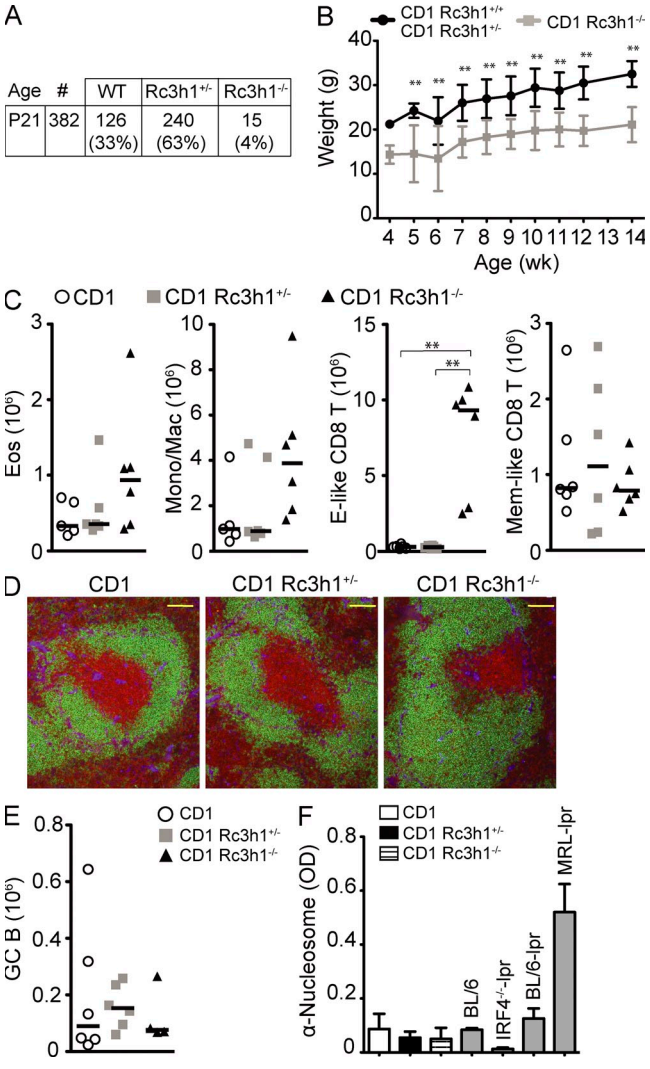

Figure 6. Roquin knockout mice can survive on a CD1 outbred genetic background. (A) Genotype frequency of offspring of heterozygous matings of CD1 $Rc3h1^{+/-}$ mice. (B) Body weight curve of $Rc3h1^{-/-}$ mice compared with control littermates (2–21 mice per group and time point). Error bars indicate SD. (C and E) Absolute cell numbers of eosinophils (Eos; $Gr1^{int}$Siglec-F^{+}), monocytic/macrophages (Mono/Mac; Siglec$F^{-}Gr1^{int}Mac1^{+}$), splenic $CD8^{+}$ T cell subsets (Effector [E]-like, $CD44^{hi}CD62L^{lo}$; memory (Mem)-like, $CD44^{hi}CD62L^{hi}$; C) and germinal center (GC; $B220^{+}PNA^{hi}Fas^{hi}CD38^{lo}$) B cells (E) calculated from six mice of the indicated genotypes. Bars represent medians. (D) Immunofluorescence of spleen sections: green, α-B220; red, α-CD3; blue, α-laminin. Bars, 100 µm. (F) Titers of autoantibodies against nucleosomes detected by ELISA in the serum of eight to nine 2.5–3.5-mo-old mice of the indicated genotypes. Columns and error bars indicate means ± SD.
**, $P < 0.001$; one-way ANOVA.

MATERIALS AND METHODS

Genetically modified mice. To generate a conditional *rc3h1* allele, we cloned a targeting vector to flank exons 4–6 with loxP sites. An Frt site–flanked neo^{R} cassette was placed in the third intron of the *Rc3h1* gene. A 4.0-kb fragment was used as the 5′ homology region, a 2-kb fragment was placed between the two loxP sites, and a 4.0-kb fragment was used as the 3′ homology region. C57BL/6 ES cells were transfected, cultured, and selected essentially as previously described for Bruce 4 ES cells (Schmidt-Supprian et al., 2000). After blastocyst injection of correctly targeted clones and transmission of the conditional allele through the germline of resulting chimeras, the Frt-flanked neo^{R} cassette was removed by using an Flpe-deleter strain. *Rc3h1*^{F}, Nestin-cre (used as deleter mice; Betz et al., 1996), Flpe-deleter (Rodríguez et al., 2000), CD4cre (Lee et al., 2001), VavCre (de Boer et al., 2003), and CD19cre (Rickert et al., 1997) were kept on a C57BL/6 genetic background. All mice analyzed were 2–4 mo old, unless otherwise indicated. CD1 outbred mice were kept at the Max Planck Institute of Biochemistry (MpiCrlIcr:CD-1). Mice were housed in the specific pathogen–free animal facility of the Max Planck Institute of Biochemistry. All animal procedures were approved by the Regierung of Oberbayern.

Flow cytometry. Single-cell suspensions were prepared and stained with monoclonal antibodies: PD-1 (J43), ICOS (7E.17G9), B220 (RA3-6B2), CD19 (eBio1D3), CD25 (PC61.5), CD38 (90), CD4 (RM4-5), CD44 (IM7), CD5 (53-7.3), CD62L (MEL-14), CD8 (53-6.7), FoxP3 (FJK-16s), GR-1 (RB6-8C5), IgD (11–26), IgM (II/41), Mac-1 (M1/70), TCR-β (H57-597), CD95 (15A7), CD21 (7G6), c-kit (2B8), KLRG1 (2F1), CD127 (A7R34), CD122 (TM-b1), Tbet (eBio4B10), F4/80 (A3-1), CD115 (AFS98), CD45RB (C363.16A; all eBioscience), Siglec-F (E50-2440), CD138 (281-2), CXCR5 (2G8), CD11c (HL3), Vα11.1/11.2 (RR8-1), Vα2 (B20.1), Vα3.2 (RR3-16), Vα8.3 (B21.14), TCR Vβ screening panel (all BD), and PNA (Vector Laboratories). Samples were acquired on FACSCalibur and FACSCantoII (BD) machines and analyzed with FlowJo software (Tree Star). To evaluate the relative ICOS expression on T cell subsets of the different cell type–specific Roquin knockout mice, four sets of three genotypes (cre control, heterozygous knockout, and homozygous knockout) were analyzed. The ICOS mean fluorescence intensity (MFI) for the cre transgenic control cells was set to 1 for each set.

Cell culture. We generated primary and SV40 large T–immortalized *Rc3h1*$^{F/F}$ and control embryonic fibroblasts and treated them by cre protein transduction with Histag-tat-NLS-cre (Peitz et al., 2007).

Western blot. To prepare whole-cell lysates, cells were lysed for 15 min on ice by RIPA buffer, 10 µg/ml aprotinin, 10 µg/ml leupeptin, 0.1 mM Na3VO4, 1 mM PMSF, 10 mM NaF, 1 mM DTT, and 8 mM β-glycerophosphate. Polyvinylidene fluoride membranes were blotted with the following antibodies: anti-Rc3h1 (Bethyl Laboratories, Inc.), antitubulin (clone YL1/2;

Millipore), antiactinin (clone AT6/172; Millipore), and anti-GAPDH (clone 6C5; EMD).

Immunofluorescence and immunohistochemistry. For immunofluorescence stainings, frozen 10-µm sections were thawed, air dried, methanol fixed, and stained for 1 h at room temperature in a humidified chamber with FITC-conjugated B220 (eBioscience), biotinylated rat anti-CD3 (BD), and rabbit antilaminin (gift from M. Sixt, Institute of Science and Technology Austria, Klosterneuburg, Austria) followed by Alexa Fluor 488–conjugated antifluorescein (Invitrogen), Cy3-conjugated streptavidin (Jackson ImmunoResearch Laboratories, Inc.), and Cy5-conjugated anti–rabbit antibodies (Jackson ImmunoResearch Laboratories, Inc.). Images were acquired using an Axio Imager.Z1 fluorescent microscope (Carl Zeiss) with AxioCam MRc5 (Carl Zeiss) and analyzed with AxioVision Rel. 4.8 software (Carl Zeiss).

Histology. Whole embryos or newborn pups were fixed for 24 h in 4% paraformaldehyde and decalcified for 4 h in Osteosoft (Merck), and heads and whole embryos were cut sagittally at the midline. Dehydration and paraffin embedding were performed using a vacuum embedding system (VIP; Sakura). Paraffin slides were performed with 4-µm thickness and stained with hematoxylin and eosin and periodic acid Schiff (PAS). Images were taken using a virtual slide microscopy system (dotslide 2.0; Olympus).

ELISA. Antinuclear autoantibodies to eight different autoantigens were detected using the Varelisa ANA 8 screen (Phadia). Serum from a 1-yr-old BXD2 mouse was used as positive control. The following ELISAs were performed as described previously (Lech et al., 2008). For antinucleosome antibodies, MaxiSorp ELISA plates (Thermo Fisher Scientific) were precoated with poly-L-lysine (Trevigen) and PBS (ratio 1:1) for 1 h. ELISA plates were washed with 50 mM Tris and 0.14 M NaCl buffer and incubated with mouse double-stranded DNA–histones (both 2 µg/ml) in SSC buffer overnight at 4°C. For anti-Smith antibodies, MaxiSorp ELISA plates were coated with Smith antigen (Immunovision) in 0.05 M carbonate-bicarbonate buffer overnight at 4°C. For rheumatoid factor, ELISA plates were coated with 10 µg/ml rabbit IgG (Jackson ImmunoResearch Laboratories, Inc.) in 0.05 M carbonate-bicarbonate buffer overnight at 4°C. Serum samples were diluted 1:10 for all IgG ELISAs. 24-wk C57BL/6 wild-type and antibody-poor (IRF-4$^{-/-}$BL/6lpr) serum was used as negative controls. C57BL/6-lpr and MRL-lpr 24-wk mouse serum was used as positive control. Specific IgGs were detected by horseradish peroxidase–conjugated goat anti–mouse IgG (Bethyl Laboratories, Inc.).

Transplantation of thymic epithelial cells. Embryonic thymic lobes (E16.5) were placed onto Isopore membrane filters (Millipore), floating on 3 ml dGuo medium (IMDM) supplemented with 1.35 mM deoxyguanosine (Sigma-Aldrich) and 10% vol/vol FCS (Invitrogen) and cultured for 5 d. After dGuo treatment, the lobes were washed in PBS and transplanted underneath the kidney capsules of athymic C57BL/6 nude mice (Taconic).

Statistics. Statistical analysis of the results was performed by one-way analysis of variance (ANOVA) followed by Tukey's test or by Student's *t* test. P-values are presented in figure legends where a statistically significant difference was found.

Online supplemental material. Fig. S1 shows the targeting strategy for the *rc3h1*^{FL} allele and ablation of Roquin in T cells. Figs. S2, S3, and S4 show the effects of T cell (Fig. S2)–, hematopoietic system (Figs. S3 and S4)–, and B cell–specific (Fig. S4) ablation of Roquin. Fig. S5 shows T cell development and selection in nude mice transplanted with *Rc3h1*$^{-/-}$ and control fetal thymic epithelial cells. Fig. S6 shows that outbred CD1 Roquin$^{-/-}$ mice display growth retardation and immune deregulation. Supplemental material and methods describe the preparation and staining of cytospins and ELISA. Online supplemental material is available at http://www.jem.org/cgi/content/full/jem.20110578/DC1.

We thank Christoph Vahl for cell sorting and Vigo Heissmeyer for advice. We are grateful to Reinhard Fässler for support. We wish to thank Julia Knogler, Barbara Habermehl, and Elenore Samson for technical assistance. We are indebted to Vigo Heissmeyer, Klaus Heger, Christoph Vahl, and Yuanyuan Chu for critical reading of the manuscript.

This study was supported by Emmy Noether grant SCHM2440 from the Deutsche Forschungsgemeinschaft (DFG) and a grant from the Thyssen Foundation to M. Schmidt-Supprian. H.-J. Anders was supported by DFG grant AN372/10-1, and M. Aichinger and L. Klein were supported by DFG grant KL1228/2-1.

The authors have no conflicting financial interests.

Submitted: 23 March 2011
Accepted: 21 July 2011

REFERENCES

Athanasopoulos, V., A. Barker, D. Yu, A.H. Tan, M. Srivastava, N. Contreras, J. Wang, K.P. Lam, S.H. Brown, C.C. Goodnow, et al. 2010. The ROQUIN family of proteins localizes to stress granules via the ROQ domain and binds target mRNAs. *FEBS J.* 277:2109–2127. doi:10.1111/j.1742-4658.2010.07628.x

Betz, U.A., C.A. Vosshenrich, K. Rajewsky, and W. Müller. 1996. Bypass of lethality with mosaic mice generated by Cre-loxP-mediated recombination. *Curr. Biol.* 6:1307–1316. doi:10.1016/S0960-9822(02)70717-3

de Boer, J., A. Williams, G. Skavdis, N. Harker, M. Coles, M. Tolaini, T. Norton, K. Williams, K. Roderick, A.J. Potocnik, and D. Kioussis. 2003. Transgenic mice with hematopoietic and lymphoid specific expression of Cre. *Eur. J. Immunol.* 33:314–325. doi:10.1002/immu.200310005

Glasmacher, E., K.P. Hoefig, K.U. Vogel, N. Rath, L. Du, C. Wolf, E. Kremmer, X. Wang, and V. Heissmeyer. 2010. Roquin binds inducible costimulator mRNA and effectors of mRNA decay to induce microRNA-independent post-transcriptional repression. *Nat. Immunol.* 11:725–733. doi:10.1038/ni.1902

Goodnow, C.C. 2007. Multistep pathogenesis of autoimmune disease. *Cell.* 130:25–35. doi:10.1016/j.cell.2007.06.033

Harris, M.J., and D.M. Juriloff. 2007. Mouse mutants with neural tube closure defects and their role in understanding human neural tube defects. *Birth Defects Res. A Clin. Mol. Teratol.* 79:187–210. doi:10.1002/bdra.20333

King, C., S.G. Tangye, and C.R. Mackay. 2008. T follicular helper (TFH) cells in normal and dysregulated immune responses. *Annu. Rev. Immunol.* 26:741–766. doi:10.1146/annurev.immunol.26.021607.090344

Kyewski, B., and L. Klein. 2006. A central role for central tolerance. *Annu. Rev. Immunol.* 24:571–606. doi:10.1146/annurev.immunol.23.021704.115601

Lech, M., O.P. Kulkarni, S. Pfeiffer, E. Savarese, A. Krug, C. Garlanda, A. Mantovani, and H.J. Anders. 2008. Tir8/Sigirr prevents murine lupus by suppressing the immunostimulatory effects of lupus autoantigens. *J. Exp. Med.* 205:1879–1888. doi:10.1084/jem.20072646

Lee, P.P., D.R. Fitzpatrick, C. Beard, H.K. Jessup, S. Lehar, K.W. Makar, M. Pérez-Melgosa, M.T. Sweetser, M.S. Schlissel, S. Nguyen, et al. 2001. A critical role for Dnmt1 and DNA methylation in T cell development, function, and survival. *Immunity.* 15:763–774. doi:10.1016/S1074-7613(01)00227-8

Linterman, M.A., R.J. Rigby, R. Wong, D. Silva, D. Withers, G. Anderson, N.K. Verma, R. Brink, A. Hutloff, C.C. Goodnow, and C.G. Vinuesa. 2009a. Roquin differentiates the specialized functions of duplicated T cell costimulatory receptor genes CD28 and ICOS. *Immunity.* 30:228–241. doi:10.1016/j.immuni.2008.12.015

Linterman, M.A., R.J. Rigby, R.K. Wong, D. Yu, R. Brink, J.L. Cannons, P.L. Schwartzberg, M.C. Cook, G.D. Walters, and C.G. Vinuesa. 2009b. Follicular helper T cells are required for systemic autoimmunity. *J. Exp. Med.* 206:561–576. doi:10.1084/jem.20081886

Peitz, M., R. Jäger, C. Patsch, A. Jäger, A. Egert, H. Schorle, and F. Edenhofer. 2007. Enhanced purification of cell-permeant Cre and germline transmission after transduction into mouse embryonic stem cells. *Genesis.* 45:508–517. doi:10.1002/dvg.20321

Rickert, R.C., J. Roes, and K. Rajewsky. 1997. B lymphocyte-specific, Cre-mediated mutagenesis in mice. *Nucleic Acids Res.* 25:1317–1318. doi:10.1093/nar/25.6.1317

Rodríguez, C.I., F. Buchholz, J. Galloway, R. Sequerra, J. Kasper, R. Ayala, A.F. Stewart, and S.M. Dymecki. 2000. High-efficiency deleter mice show that FLPe is an alternative to Cre-loxP. *Nat. Genet.* 25:139–140. doi:10.1038/75973

Schmidt-Supprian, M., W. Bloch, G. Courtois, K. Addicks, A. Israël, K. Rajewsky, and M. Pasparakis. 2000. NEMO/IKK gamma-deficient mice model incontinentia pigmenti. *Mol. Cell.* 5:981–992. doi:10.1016/S1097-2765(00)80263-4

Vinuesa, C.G., M.C. Cook, C. Angelucci, V. Athanasopoulos, L. Rui, K.M. Hill, D. Yu, H. Domaschenz, B. Whittle, T. Lambe, et al. 2005. A RING-type ubiquitin ligase family member required to repress follicular helper T cells and autoimmunity. *Nature.* 435:452–458. doi:10.1038/nature03555

Yu, D., and C.G. Vinuesa. 2010. Multiple checkpoints keep follicular helper T cells under control to prevent autoimmunity. *Cell. Mol. Immunol.* 7:198–203. doi:10.1038/cmi.2010.18

Yu, D., A.H. Tan, X. Hu, V. Athanasopoulos, N. Simpson, D.G. Silva, A. Hutloff, K.M. Giles, P.J. Leedman, K.P. Lam, et al. 2007. Roquin represses autoimmunity by limiting inducible T-cell co-stimulator messenger RNA. *Nature.* 450:299–303. doi:10.1038/nature06253